JJMIE

Volume 17, Number 1, March 2023
ISSN 1995-6665
Pages 69 – 85

Jordan Journal of Mechanical and Industrial Engineering

Impact of Internal Wall Barriers on Airflow Pattern in Natural Cross-Ventilation of the Common Houses in Bhubaneswar City, India

Soma Kalia[1*], Nibedita Mishra[2], Prakash Ghose[3]

[1]Department of Home Science, Ramadevi University, Bhubaneswar-751007, India
[2] Department of Home Science, Puri Woman's college, Ramadevi University, Bhubaneswar-751007, India
[3]School of Mechanical Engineering, KIIT Deemed to be University, Bhubaneswar-751024, India

Received 20 Sep 2022 Accepted 19 Jan 2023

Abstract

Common walls between houses are a major reason for improper ventilation in apartment buildings. They make a compulsion for improper positioning of doors/windows. The shape of the house also affects the airflow distribution patterns inside the house. In this work, the effect of various shapes of the house on the ventilation inside the rooms is investigated with a cross-flow ventilation configuration, where the total floor area of the house is maintained as 1000 square feet. Moreover, work also has been performed to investigate the airflow inside a square-shaped house with different door/window configurations for various inlet airflow directions. Besides that, the impact of inlet airflow velocity on the ventilation process has also been investigated. From the investigation, it has been observed that with an increase in air volume flow rate, the area covered with low-velocity air (< 1 m/s) decreases and the area covered with high-velocity air (> 2 m/s) increases irrespective of the shape of the house but does not follow any pattern for the comfort condition airflow velocity. The airflow pattern is not changed significantly with increase in inlet airflow velocity, but the airflow velocity regions are changed significantly. For a square shape house, 78% area is covered with a low air velocity region (< 1 m/s) is the highest with N & E door/window configuration. 62% area covered with high air velocity region (> 2 m/s) is the highest with N & S door/window configuration. 26% area covered with comfort flow condition (between 1-2 m/s) is the highest with N & S door/window configuration.

Keywords: Natural ventilation, door/window position, comfort air velocity.

1. Introduction

Ventilation is a process of continuous replacement of used air with fresh natural air from a room, building or confined space. The ventilation process refers to natural ventilation when the airflow occurs by natural means. It may be through ambient airflow due to the pressure difference between outside and inside air or may be due to the temperature difference between occupants and inside room air or both. On the other hand, in mechanical ventilation, airflow is driven by the mean of pumps, blowers, etc. Proper ventilation must be required to maintain the necessary oxygen level, remove pollutant air, remove odour and smoke and control temperature and humidity in an inhabited area. Natural ventilation does not require any running cost, and it has been observed that the total energy consumption of a typical residential building is reduced by up to 40% when only natural ventilation is preferred [1]. Apart from ventilation, the conversion of wind energy potency to renewable energy is an emerging area of research[2]. However, in order to obtain a proper ventilating effect naturally, the house design, housing direction, neighbourhood barriers and proper positioning of doors and windows, considering seasonal wind flow direction, temperature and humidity, are the most important factor of concern. However, these factors are being considered by architects since the beginning of human civilization, but their effect through proper scientific experiments are being used for the last few decades. Generally, ventilation effects are investigated with the help of wind tunnels through model testing experimentally[3-5].Tecle et al. [6]conducted experiments to investigate wind-driven ventilation for various door window positions and different percentages of door window openings. Single wall window configuration crossed flow window configuration and adjacent wall window configuration cases are investigated by them for 36 different wind directions. Cho et al. [7] suggested increasing the effectiveness of ventilation through proper window opening area, and positioning of windows with respect to the elevation of high-rise buildings through experimentation. Omrani et al. [8] experimentally compared the effectiveness of cross ventilation over single-side ventilation through in-situ measurements. In their study, mainly day-wise summer weather condition is

* Corresponding author e-mail: somakalia7@gmail.com.

included and it has been observed that more than 70%time the room condition is under standard comfort zone with cross ventilation arrangement, whether with single side ventilation, it is nearly 1%.Kyritsi and Michael[9] investigated the window and door opening strategy for the whole day and night during summer for cross-ventilated houses and single-side ventilated houses in Nicosia city, Cyprus. Dascalaki et al.[10] developed a mathematical model for the prediction of airflow rate in single-sided ventilated houses. In this study, the ventilation parameter data of 52 single-sided ventilated houses are used to develop the model. Hawendi et al.[11]investigated the effect of boundary wall height on the airflow pattern inside a single-side ventilated house. They reported that house with boundary wall offer better ventilation than those without boundary wall because it provides a favorable direction to the wind toward the door. It is also mentioned that an increase in boundary wall height as compared to standard boundary wall height does not give any significant improvement to the ventilating effect inside the house. Zhang et al. [12] investigated the impact of cross flow on various internal, external opening configuration of a generic building. It is reported that two opening configuration is the most efficient for cross flow ventilation. Different opening size for inlet and outlet side provides complete airflow inside the room as compared to same inlet and outlet opening size. Zhiyi et al. [13] studied the natural ventilation of a typical apartment house for Chinese climatic condition. They introduced channel connections for the ventilation. It is found that horizontal flow channel improves the air flow particularly for the leeward south side apartment.

Many authors used Computational Fluid Dynamics (CFD) as a tool to study natural ventilation [14-16]. Derakhshan and Shaker [17]performed a computational simulation on natural ventilation in an existing house and reported that small changes in window dimensions and their vertical and lateral positions enhance effective ventilation. Moreover, when wind direction becomes greater than 45º, the ventilation becomes good enough irrespective of window position and dimension. Liu et al. [18] employed both experimentation and CFD to investigate the ventilation in a cross-ventilated arrangement house and airflow around the building as well. It is reported that a 24.4% error has been observed in CFD prediction with standard boundary conditions. With modified boundary conditions, CFD simulation prediction is satisfactory. Moreover, it is indicated that RNG k-ε turbulent model could not predict the flow separation precisely. King et al. [19]investigated the influence of neighbouring building orientations on ventilation. In this work, the performance of the Ansys Fluent and OpenFOAM CFD tools were also compared and reported that both are good enough to predict the flow behaviour. It has been mentioned that when the orientation angle is higher that 195º, the ventilating effect inside the desired house is maximum with a cross ventilation configuration. Investigation on single-sided ventilation becomes much more relevant when space constraints area concern. Visagavel and Srinivasan [20] used CFD to investigate the ventilation effect with cross-ventilation configuration, single-sided leeward and windward configuration by varying the opening area. It is mentioned that, though cross ventilation is much more effective, further investigation on single-sided ventilation is necessary, because, in a country like India, so many buildings are constructed with single-side ventilation provision due to space constraints.Wang et al. [21] computationally evaluated the performance of several types of windows according to their opening configurations with single-sided arrangements through buoyancy-driven flow. They used RANS based k-ω turbulent model to account for the turbulent effect. It has been reported that the single constant discharge coefficient is not acceptable for different buoyancy and flow area. Moye et al. [22] also used SST k-ω turbulent model in their computational model. Where the effect of gable roof angle on natural ventilation for an isolated building is investigated. It has been observed that a higher roof pitch of gable roof building is should be preferred for better ventilation rate. Allocca et al. [23] worked on single-sided natural ventilation considering the bouncy effect. They reviled that CFD simulation underpredicted by 25% from the measured value. Moreover, no guiding rules could be established for predicting the occurrence of counteracting wind and stack effects, since no consistent trends were observed. k-ε turbulent model, Reynolds stress turbulent model and Large eddy simulation turbulent models are also frequently used to incorporate the turbulence effect in flow inside or over a domain[24-30].

From the literature, it is observed that no work has been performed to determine the comfort airflow region (air velocity between 1-2 m/s) for different shapes of the house with various door/window configurations when air with different velocities enters through various directions. This work is segregated into two parts. In the first part, the effect of cross ventilation has been studied on the airflow distribution inside the spaces of various shapes of houses. In the second part, two side ventilation effects on the airflow distribution for a square shape flat have been investigated. Mainly the percentage of the area coming under comfort airflow velocity (1-2 m/s) has been evaluated for different airflow velocities, which havenot been yet investigated by any researcher. For this, several 2-D CFD simulations have been performed. The performances of the computational models used are verified with an in-house wind tunnel experiment.

2. Physical model

In this study, a few hypothetical flat models are considered for the investigation of wind flow in different spaces inside the house. In the first part of this work, an investigation of airflow distribution in three different shapes of the flats (Rectangular shape, square shape and L-shape) is considered, where the floor area of every flat is taken as 1000 square ft. The floor plans of the flats are given in figure 1.

In this part of the work, only cross-ventilation is considered. Irrespective of the shapes of the plan, a total of four windows and two small windows on the bathroom walls are used. Moreover, the main entrance door is kept on the south side irrespective of the shape of the house. The dimensions of the windows and doors are taken according to standard architectural size as given in table 1.

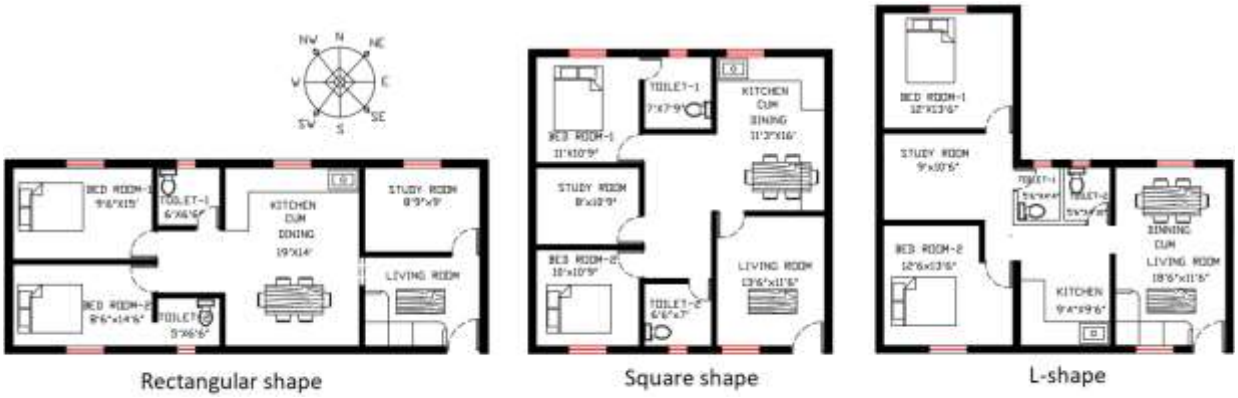

Figure 1. Physical plan of flats with various shapes with cross-flow configuration

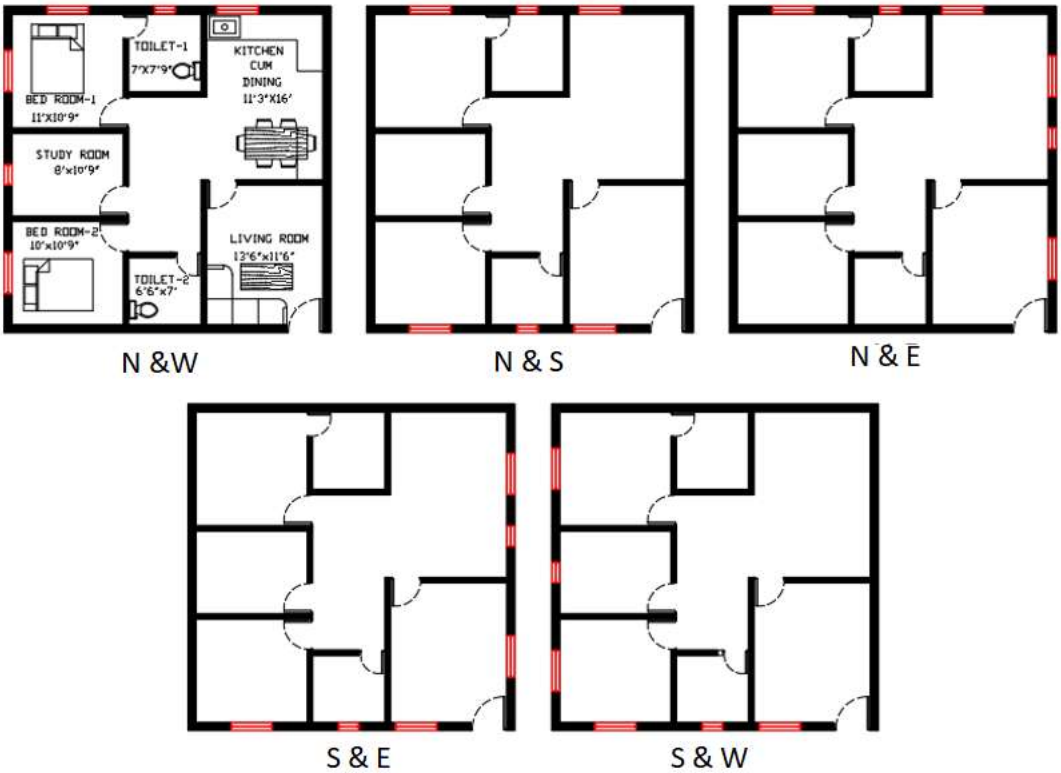

Figure 2. Physical plan of square shape house for different door/window orientations

In the second part of the work, the investigation on airflow distribution in the house has been carried out for square shape plan only, where the windows are placed only on two sides and the remaining two sides are closed by assuming that these are common walls between the buildings. However main entrance door is kept on the south side irrespective of cases. Figure 2 shows the window positions. Here a total of four windows are used for ventilation including two small windows on the bathroom wall.

Table-1 Dimensions of door and windows

Items	Total number	Dimension width (ft& inch)
Main door	1	3’6”
Room door	4	3’
Bathroom door	2	2’6”
Window	4	4’
Bathroom window	2	2’

The air velocity that is required as a boundary condition for simulations is taken from the year-round weather data of Bhubaneswar city. Monthly average eleven-year weather data (2010-2020) such as; wind velocity, wind direction, dry bulb temperature and relative humidity are collected from the weather online web portal www. weatheronline.com [31]. Figure 3 shows the location of Bhubaneswar city, India situated at 20.2961° N, 85.8245° E. Figure 4(a) shows the monthly average wind velocity of each month for 11 years. Similarly, figure 4 (b) illustrates the average wind velocity of 11 years, month-wise. It has been observed that the average wind velocity is the highest (around 16 km/hr) in April and May, whereas, in the winter season (December and January), the wind velocity is around 4 km/hr. Therefore, for the simulation, the wind velocity is used within the range of 4-16 km/hr.

Figure 3. Location of Bhubaneswar city, India on map

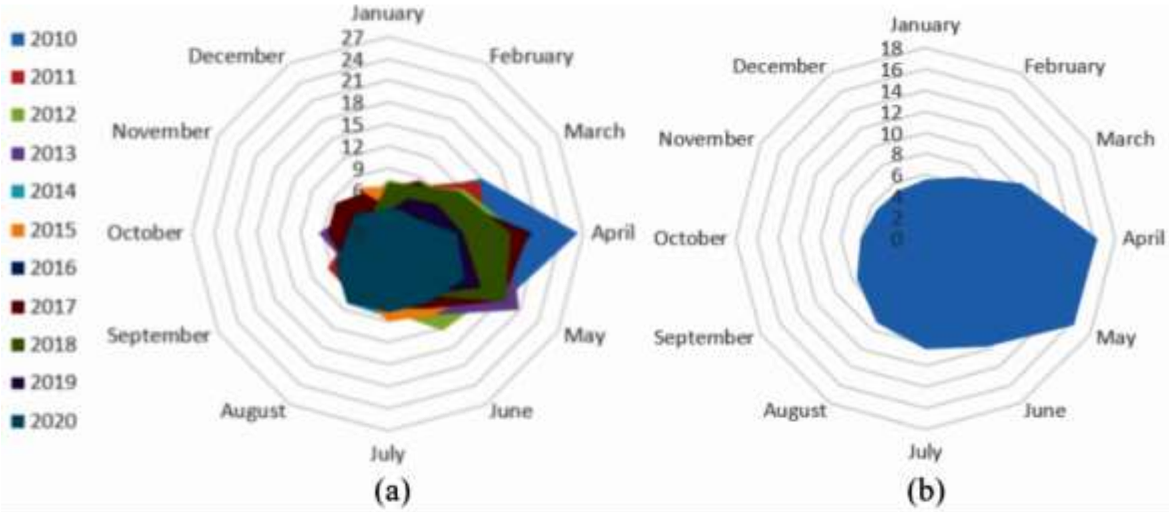

Figure 4. Wind velocity (km/hr) (a) Monthly average wind velocity of each month for 11 years (b) Average wind velocity of 11 years, month-wise.

3. Computational modelling

This is a simple cold flow problem. Bouncy-driven airflow is neglected here. Therefore, only conservation of mass and momentum equations are solved to obtain pressure and velocity distribution. Since the problem is turbulent in nature, time-averaged mass conservation and RANS equations are solved. In order to evaluate the Reynolds stresses, the Boussinesq equation is used. For the evaluation of eddy viscosity required to solve Boussinesq, the standard k-ε turbulent model is used. The governing equations are given as follows;

Conservation of mass

$$\frac{\partial}{\partial x_i}(\rho \bar{u}_i) = 0 \qquad (1)$$

Conservation of momentum

$$\frac{\partial}{\partial x_i}(\rho \bar{u}_i \bar{u}_j) = -\frac{\partial \bar{p}}{\partial x_i} + \frac{\partial}{\partial x_j}\left(\bar{\tau}_{ij} - \rho \overline{u_i' u_j'}\right) \qquad (2)$$

where, ρ is the density of the fluid and $\bar{u}_i$ and $\bar{p}$are the time average mean flow velocity and time average mean pressure. The stress tensor in the momentum equation is expressed as.

$$\bar{\tau}_{ij} = \mu\left(\frac{\partial \bar{u}_i}{\partial x_j} + \frac{\partial \bar{u}_j}{\partial x_i}\right) \qquad (3)$$

$-\rho\overline{u_i' u_j'}$is the Reynolds stress and it is an additional term that has been formed due to time averaging.

Two transport equations are solved to obtain the rate of generation of turbulent kinetic energy (k) and dissipation rate of turbulent kinetic energy (ε), respectively. The assumption for this model is that the flow is fully turbulent (high Reynolds number). In the standard k-ε model, the governing equations for k and ε are expressed as follows:

$$\frac{\partial}{\partial x_i}(\rho k \bar{u}_i) = \frac{\partial}{\partial x_j}\left[\left(\mu + \frac{\mu_t}{\sigma_k}\right)\frac{\partial k}{\partial x_j}\right] + G_k + \rho\varepsilon \qquad (4)$$

$$\frac{\partial}{\partial x_i}(\rho \varepsilon \bar{u}_i) = \frac{\partial}{\partial x_j}\left[\left(\mu + \frac{\mu_t}{\sigma_\varepsilon}\right)\frac{\partial \varepsilon}{\partial x_j}\right] + C_{1\varepsilon}\frac{\varepsilon}{k}G_k - C_{2\varepsilon}\rho\frac{\varepsilon^2}{k} \qquad (5)$$

In the above equations, G_k represents the generation of turbulent kinetic energy, which is expressed in terms of the mean velocity values as,

$$G_k = \left(\mu_t\left(\frac{\partial \bar{u}_i}{\partial x_j} + \frac{\partial \bar{u}_j}{\partial x_i}\right) - \frac{2}{3}\rho k \delta_{ij}\right)\frac{\partial \bar{u}_j}{\partial x_i} \qquad (6)$$

Turbulent viscosity can be obtained from the dimensional analysis as given below

$\mu_t = C\rho\rho v l = C_\mu \rho \frac{k^2}{\varepsilon}$, where$C_\mu$ a model constant and its value is taken as 0.09.

$v = k^{1/2}, l = \frac{k^{3/2}}{\varepsilon}$, where v is the velocity scale and l is the length scale

The model constants $C_{1\varepsilon}$, $C_{2\varepsilon}$, σ_k(turbulent Prandtl number for k) and σ_ε (turbulent Prandtl number for ε) in the k and ε equations have default values obtained empirically.

3.1. Model validation and grid independence test

For experimentation, a scaled model (scale ratio 1:50) of the square shape geometry with cross-flow door/window configuration is prepared with the help of a 3-D printing machine. Reynolds number ($Re = \frac{\rho V D_h}{\mu}$)for inflow velocity V=1.11 m/s is evaluated first. In Reynolds number,ρ and μ are the density and viscosity of air at STP (standard temperature and pressure). The hydraulic diameter of doors/windows on the south side is evaluated as; ($D_h = 4A/P$). The scaled model hydraulic diameter is 50 times smaller than the actual house. Hence using the hydraulic diameter of the scaled model and using the evaluated Reynolds number for the actual house, the air inflow velocity of the model test is calculated as 50.08 m/s. After that, with the help of a subsonic wind tunnel, the model test is performed. Further, a scaled model geometry is prepared in Ansys fluent, and simulation is conducted following the same conditions used in the wind tunnel test. In experimentation, the velocity at different points is measured with hot-wire anemometer. The experiment setup is shown in Figures5 (a) & (b). The velocity variation along the center line connecting north and south as given in the figure shows the comparison between the experiment and simulation. As both the results are pretty closer to each other as shown in figure7, therefore, the computational models used in the simulation are hereby validated properly.

All the geometries have meshed with a quadrilateral structured grid of different cell sizes. The grid independence study has been conducted on the square-shaped geometry with cross-flow door/window orientation. The geometry is discretized with 20377, 33468, 40888 and 54265 numbers of elements. The geometry of various shapes (rectangular, square and L-shape) with mesh is shown in figure 6. Near the wall, fine mesh is created to simulate the proper effect of boundary layer formation. For this, the airflow direction is kept from south to north with an inlet airflow velocity of 1.11 m/s. The velocity variation along the center line connecting north and south is given in fig.7. From figure 7, it has been observed that there is not much variation in results obtained with 40888 and 54265 element numbers. However, to reduce the computational cost, 40888 element mesh is used for simulation. The accuracy assessment of the computational model is given in table 2. It has been observed that the computational results obtained from the 40888 element domain is deviated from the experimental results within a range of -13.77% to 19.77%.

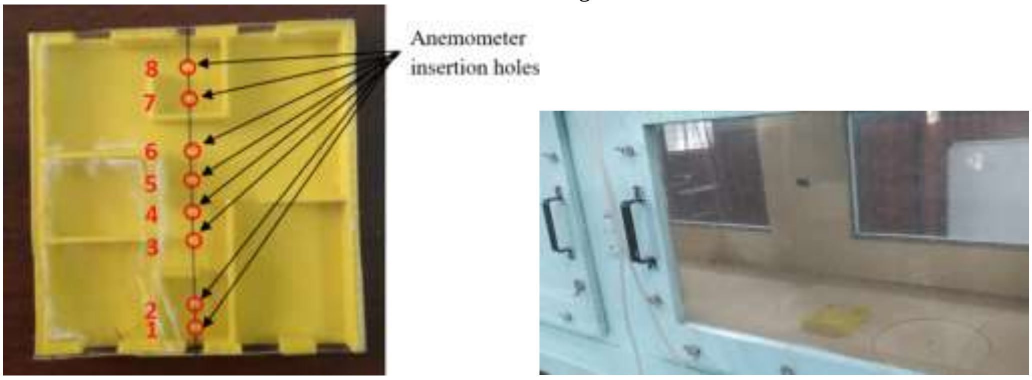

(a) (b)

Figure 5. (a) 3-D printed square shape cross ventilated house model (b) Testing in the subsonic wind tunnel

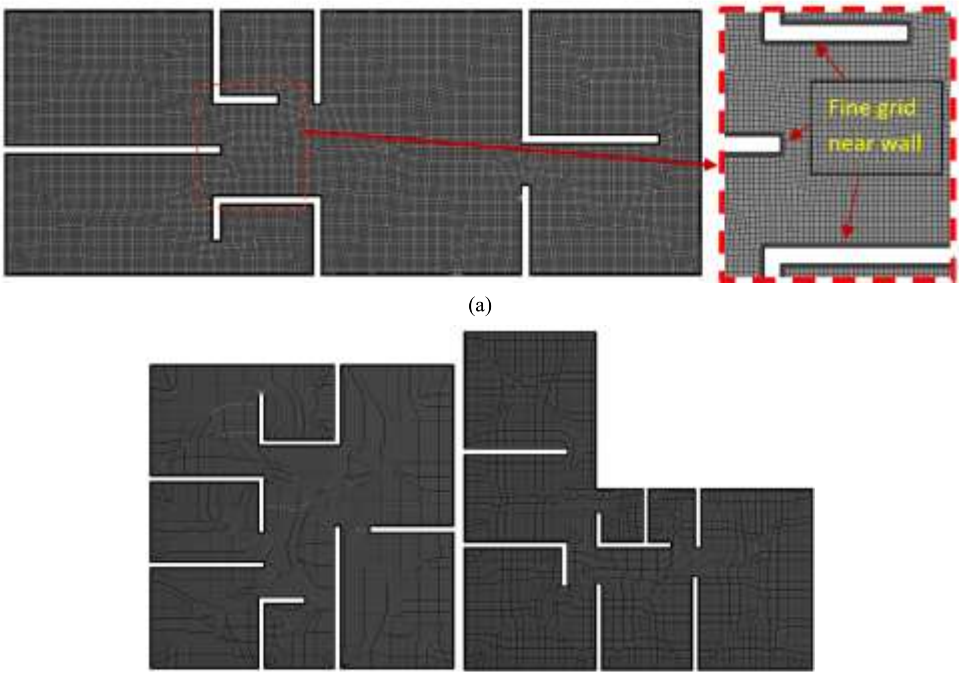

(a)

(b) (c)

Figure 6. Mesh for (a) rectangular shape house (b) square shape house (c) L-shape house

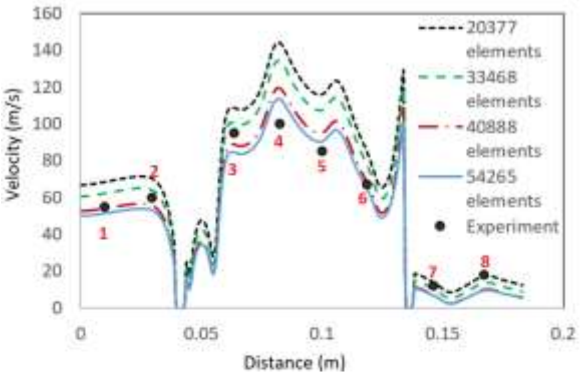

Figure 7. Grid-independent test and experimental validation

Table 2. Accuracy assessment of computational model

Location	Velocity in m/s (Experiment)	Velocity in m/s (40888 elements computational domain)	Percentage error corresponding to Experimental results
1	55	52.538	9.02%
2	60	55.502	11.90%
3	95	88.853	10.92%
4	100	119.458	-13.77%
5	85	95.157	-6.61%
6	67	67.714	3.74%
7	12	9.626	19.77%
8	18	15.628	13.05%

3.2. Boundary conditions

From Figures4 a and b, it is evident that the airflow direction varies with respect to month and the year-round average airflow velocity varies between 4 km/hr to 16 km/hr. Therefore in this work, the effect of wind flow direction and velocity on comfort zone airflow inside the house has been investigated. The information related to boundary conditions for simulations is enlisted in table 3 and the boundary condition values are given in the result discussion part.

Table 3. Boundary type and their mathematical conditions

Boundary	Type	Condition	Generation of turbulent kinetic energy (k)	Dissipation of turbulent kinetic energy (ε)
Inlet	Velocity inlet	Normal to boundary	Turbulent intensity	Hydraulic diameter
Wall	No slip wall	Friction factor	$\frac{dk}{dy} = 0$	$\frac{d\varepsilon}{dy} = 0$
Outlet	Pressure outlet	Constant gradients of variables	Turbulent intensity	Hydraulic diameter

The volume flow rate into the house for different shapes of the house and directions are given in table 4. The volume of airflow rate into the house from various directions in m^3/s per unit height of door/window for a square shape house with different door/window orientations is given in table 5. The total volume flow rate gets into the house is calculated as;

$$Q = \sum_{n=1}^{n} (W \times H)V \quad (7)$$

Where W is the width of the door/window placed on the south side when wind flows from south to north and vice versa. H is the height of the door/window. However, in this work, the value of H is taken as 1 because the volume flow rate is evaluated per unit height of the door/ window. V is the velocity of the wind.n is the number of doors/windows. The sizes of the doors and windows are given in table 1.

Table 4 Air flow volume rate into the house in m^3/s per unit height of door/window for different shapes of the house

Wind flow direction	Air flow volume rate into the house in m^3/s per unit height of door/window		
	Rectangle shape	Square shape	L-shape
Airflow direction from South to North	9.642	13.702	11.672
Airflow direction from North to South	14.209	13.702	12.179

Table 5. Air flow volume rate into the house from various directions in m^3/s per unit height of door/window for a square shape house with different door/window orientation

Wind flow direction	Inlet flow velocity	Air flow volume rate into the house in m^3/s per unit height of door/window				
		N & W	N & S	N & E	S & E	S & W
From East	1.11 m/s (4 km/hr)	NA	NA	NA	3.383	3.383
	2.22 m/s (8 km/hr)	NA	NA	NA	6.766	6.766
	3.33 m/s (12 km/hr)	NA	NA	NA	10.149	10.149
	4.44 m/s (16 km/hr)	NA	NA	NA	13.533	13.533
From West	1.11 m/s (4 km/hr)	3.383	NA	3.383	NA	NA
	2.22 m/s (8 km/hr)	6.766	NA	6.766	NA	NA
	3.33 m/s (12 km/hr)	10.149	NA	10.149	NA	NA
	4.44 m/s (16 km/hr)	13.533	NA	13.533	NA	NA
From North	1.11 m/s (4 km/hr)	3.383	3.383	3.383	NA	NA
	2.22 m/s (8 km/hr)	6.766	6.766	6.766	NA	NA
	3.33 m/s (12 km/hr)	10.149	10.149	10.149	NA	NA
	4.44 m/s (16 km/hr)	13.533	13.533	13.533	NA	NA
From South	1.11 m/s (4 km/hr)	1.184	5.022	1.184	5.022	5.022
	2.22 m/s (8 km/hr)	2.368	9.144	2.368	9.144	9.144
	3.33 m/s (12 km/hr)	3.552	13.702	3.552	13.702	13.702
	4.44 m/s (16 km/hr)	4.736	18.269	4.736	18.269	18.269

Due to the geometrical constraints, four openings are provided on the north side for rectangular shape and L-shape houses. Therefore the volume flow rate in these shapes of the houses is more when the flow direction is from north to south. On the other hand, for a square shape, the volume flow rate of air is the same irrespective of the directions of flow.

4. Results and discussion

4.1. low pattern inside the house of different shapes

Figure 8 shows the airflow pattern inside the house (left) and airflow velocity region; less than 1 m/s (represent in green colour), between 1-2 m/s (represent in brown colour) and higher than 2 m/s (represent in blue colour) inside the house (right) of various shapes when the airflow direction is from south to north. Similarly, figure 9 shows when the airflow direction is from north to south. In these simulations, the airflow velocity is taken as 12 km/ hr (3.33 m/s). To evaluate the percentage area covered with the velocity distribution < 1 m/s, in between 1-2 m/s and > 2 m/s, iso-clip areas are drawn with three different colours. Then the image is processed through the web portal www. coolphptools.com [32].

From fig.8, it has been observed that in a rectangular shape building, the maximum fraction of the air that enters through the main door, comes out through the study room window due to the front-to-front configuration. Similarly, a maximum fraction of the air that enters through the south side toilet and bedroom, comes out through the kitchen window. Here, the separating wall between the two bedrooms provides a favorable direction for the air toward the kitchen window. More interestingly, though, the north side window and north side toilet windows are given as outlet boundaries, but a small amount of air enters into the room instead of going out. Here, the high velocity of the air stream started from the south side room window and the toilet window develop a negative pressure followed by Bernoulli's principle. As a result, the air is sucked into the north side bedroom and toilet through their windows. The black arrow in this fig. 8 shows the air inlet, the red arrow shows the air outlet and a single green arrow shows the reverse flow direction. The red lines represent the major flow path of direct flow and the green line represents the reverse flow path. On both sides of the flow paths, one can visualize the circulations from the vector arrowheads. From the colour contour of this figure 8,referring to its contour legend, one can see the velocity distribution inside the room.

The right side part of this fig.8 depicts the comfort airflow region (air velocity in between 1-2 m/s), the air velocity higher and lower than the comfort condition as well. It is observed that the entire region of the north side bedroom and toilet are poorly ventilated, even the dining space as well, where the flow velocity is less than 1 m/s. In contrast, the region closer to the main flow path have an air velocity higher than 2 m/s. The major region on the east corner of the south side bedroom and study room is coming under the comfort airflow zone. Both the east and west part of the kitchen is seems to be well-ventilated.

For square shape building, airflow from south to north, two main path lines from the south side bedroom window and toilet window are merged at the middle open space of the house and released through the north side bedroom window. Similarly, the two main path lines from the living room window and main entrance door are merged in the middle open space of the house and released through the kitchen window. Here due to an adverse pressure gradient created by the main flow path, a small fraction of air enters into the north side toilet through its window. Here also, besides the main flow paths, circulation zones are observed. A strong recirculation zone is observed in the kitchen/dining room. In this case, the air velocity is higher than 2 m/s in a major portion of the house. On the other hand, the study room and the north side toilet have poor ventilation, where a major portion of the room is with a velocity of less than 1 m/s.

For the L-shape house, a major portion of the air that enters through the south side bedroom comes out through the north side bedroom window. Here, the west side toilet wall provides a favorable direction to the main flow. However, a small fraction merges with the flow line which started from the living room window. The major fraction of air that enters through the living room door moves out through the dining room window and the major fraction of air that enters through the living room window moves out through the east side toilet window. Similarly here also the circulation zones are observed beside the main flow line. A backflow is observed at the west side toilet. Here, the kitchen area and west side toilet are poorly ventilated and the living/dining space and south side bedroom seem to be well ventilated. The remaining area is over-ventilated.

Figure 9 a-c shows the ventilation pattern and comfort region for three shapes of the house when the flow becomes reversed (north to south). From the flow path lines in all three shape houses; rectangular, square and L-shape, it is observed that circulation zones are developed on both sides of the main flow paths. In a rectangular shape house, a major fraction of air enters through the north side bedroom window and comes out through the south side window. On the other hand, the remaining inlet air comes out through the main entrance door. A small amount of reverse flow air is observed at the south side toilet due to adverse pressure caused by the nearer main flow path. In square shape house, the whole inlet air from the north side windows moves out through the south side windows and a backflow air enters through the main entrance door. In the L-shape house, the air enters through the north side bedroom window and the north-west side toilet merged and moves out through the south side bedroom window. On the other hand, the air enters through the dining room window and the northeast side toilet merged and moves out through the living room window and main entrance door. Here backflow is not observed. Hence low-velocity air region is very less.

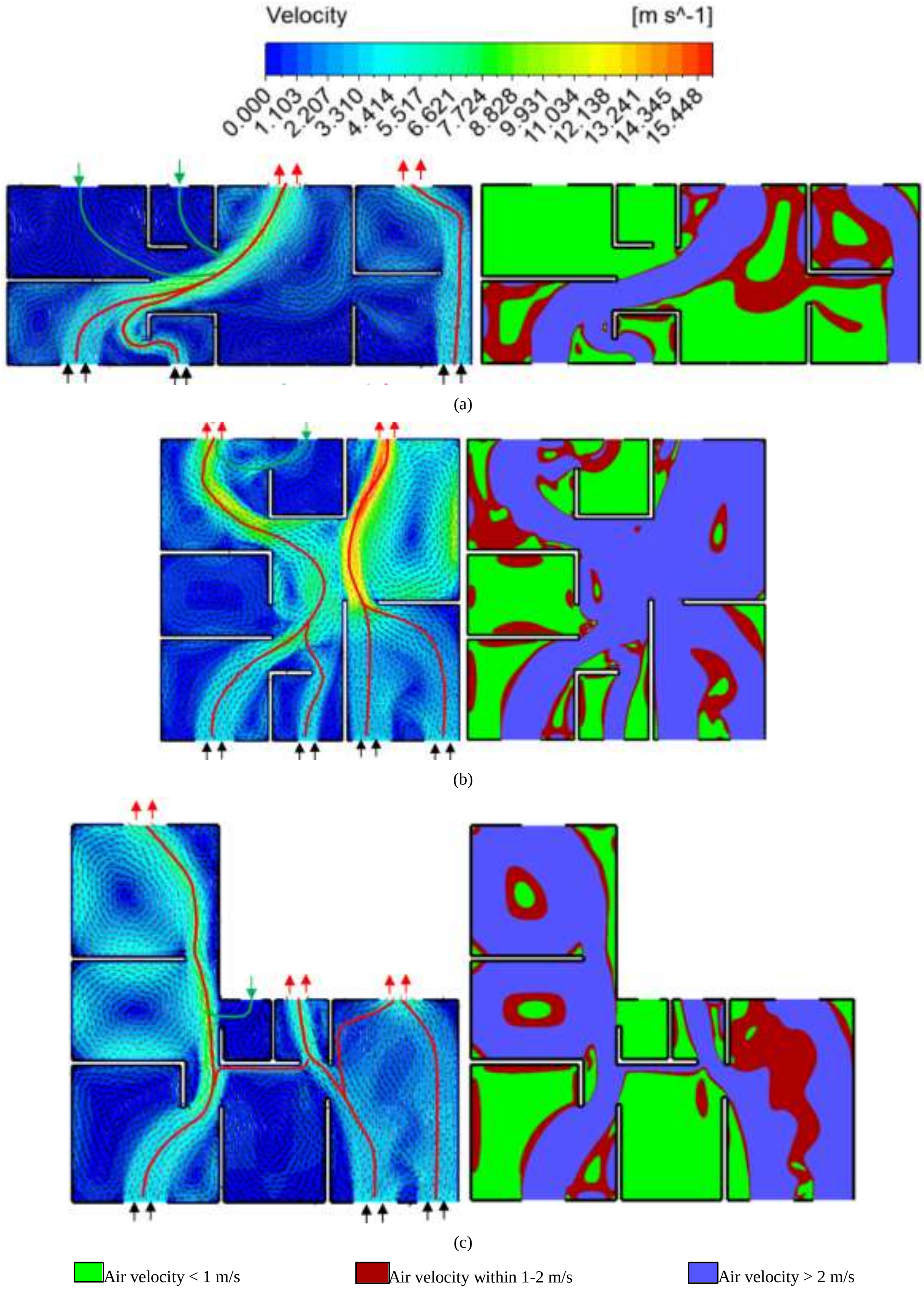

Figure 8. Air flow pattern inside the house (left) and airflow velocity region; less than 1 m/s (***green***), in between 1-2 m/s (***brown***) and higher than 2 m/s (***blue***) inside the house (right) of various shapes when the airflow direction is from south to north (a) Rectangular shape house (b) Square shape house (c) L-shape house

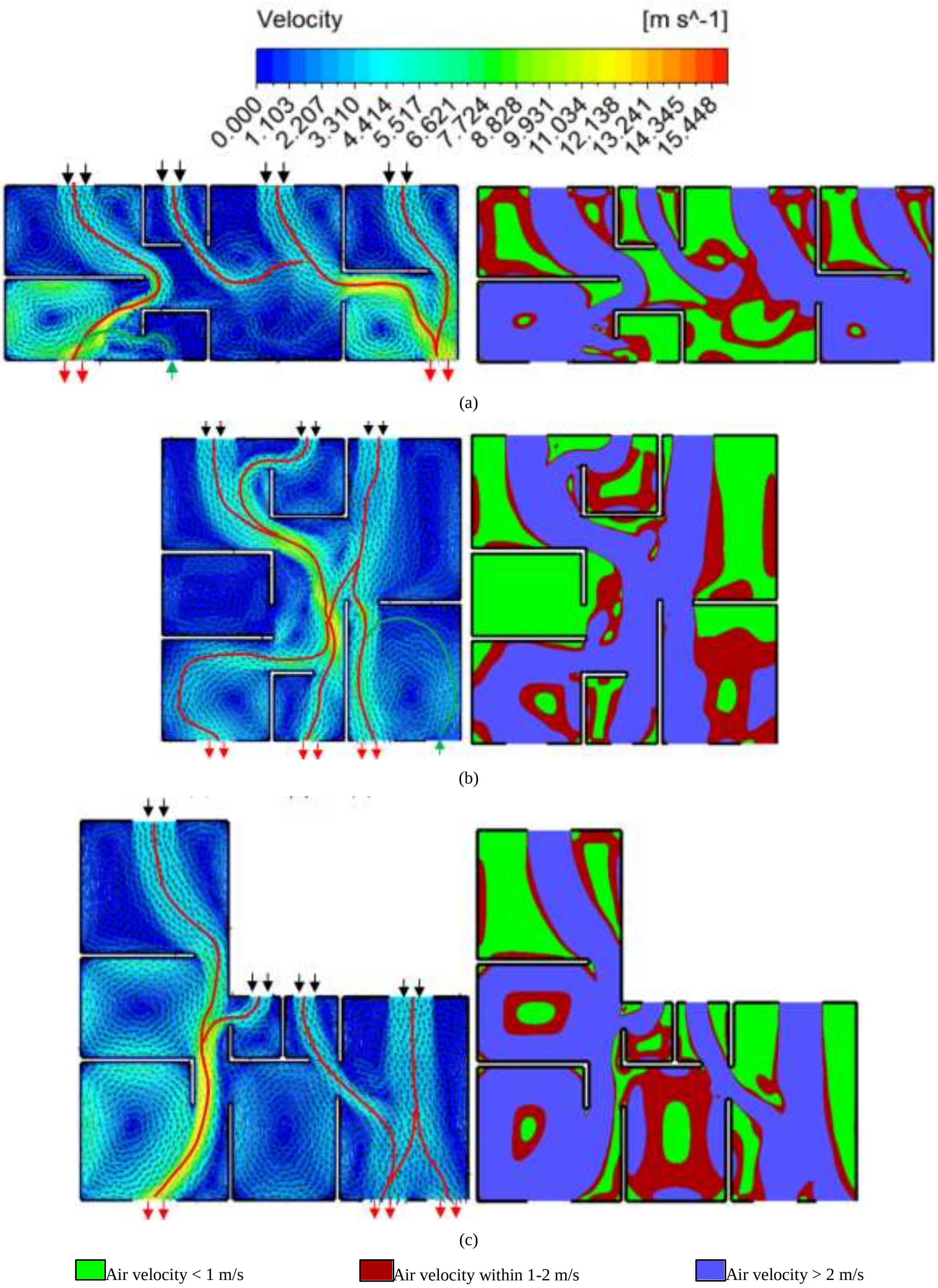

Figure 9. Air flow pattern inside the house (left) and airflow velocity region; less than 1 m/s (***green***), in between 1-2 m/s (***brown***) and higher than 2 m/s (***blue***) inside the house of various shapes (right) when the airflow direction is from north to south (a) Rectangular shape house (b) Square shape house (c) L-shape house

In Table 6, the airflow velocity covered the area in percentage inside the house of various shapes with cross flow door/window orientation are enlisted. From the right side parts of fig.8 and 9, one can visualize the same. When the wind flow direction is from south to north, the comfort condition airflow zone is around 20% in the rectangular shape house, which is the highest as compared to the other two shapes of houses. For square shape houses, it is the least (13%). In contrast to that, the air velocity region higher than 2 m/s is around the highest (around 63%) for square shape houses. For a rectangular shape house, the low-velocity area is around 52%, which is the highest among all shapes.

When the flow is revered, the comfort condition airflow zone is around 22% in the square shape house, which is the highest as compared to the other two shapes of houses. At the same time, this shape also has the highest low-velocity air flow (< 1 m/s) region (31%). The high airflow velocity (> 2 m/s) region is around 57% and 58% for rectangular and L-shape houses.

Figure 10, shows the effect of inflow air velocity on proper ventilation inside houses of different shapes when the airflow is from south to north with a cross-flow configuration. The flow pattern is not affected much by the change in inflow velocity, but the comfort airflow condition zone significantly varies with the variation of inflow velocity. From the fig.10 it can be observed, irrespective of shape, the high flow velocity region (> 2 m/s) increases with an increase in flow velocity and at the same time, the poorly ventilated area (< 1 m/s) decreases. The actual airflow velocity covered the area in percentage inside the house is shown in fig.11. For rectangular shapes, the airflow velocity region less than 1 m/s is covered by 82% of the total area when the inflow velocity is 1.11 m/s. Similarly with inflow velocity of 2.22 m/s, 3.33 m/s and 4.44 m/s the percentage area of low velocity (<1 m/s) covered is 65%, 52% and 42% respectively. A similar decreasing trend can be observed in fig.11 for the other shaped houses. For rectangular shapes, the airflow velocity region greater than 2 m/s is covered by 5% of the total area when the inflow velocity is 1.11 m/s. Similarly with inflow velocity of 2.22 m/s, 3.33 m/s and 4.44 m/s the percentage area of high velocity (>1 m/s) covered is 24%, 28% and 41% respectively. A similar decreasing trend can be observed in fig.11 for the other shaped houses.

With increase in inflow air velocity, the area covered with comfort airflow condition (1 < velocity < 2) does not follow any trend for rectangular and L-shape houses. Whereas, in square shape houses, with increase in air flow velocity, the area covered with comfortable airflow conditions decreases. For this, the highest value is 28% for the inflow air velocity of 1.11 m/s. For rectangular shape houses, the highest area covered with comfort airflow condition is 20% for the inflow air velocity of 3.33 m/s and the lowest is 11% for the inflow wind velocity of 2.22 m/s. Similarly, for L- shape houses, the highest area covered with comfort airflow condition is 29% for the inflow air velocity of 2.22 m/s and the lowest is 11% for the inflow wind velocity of 4.44 m/s.

Table 6. Airflow velocity covered the area in percentage inside the house of various shapes of the houses with cross-flow door/window orientation

Airflow velocity inside the house	Wind flow direction	Airflow velocity covered the area in percentage inside the house of various shapes		
		Rectangle shape	Square shape	L-shape
Less than 1m/s	From South to North	52%	24%	29%
In between 1-2 m/s (Comfort condition)		20%	13%	15%
Greater than 2 m/s		28%	63%	56%
Less than 1m/s	From North to South	26%	31%	21%
In between 1-2 m/s (Comfort condition)		17%	22%	21%
Greater than 2 m/s		57%	47%	58%

4.2. Flow pattern in square shape house for different wind flow directions

Figure 12 shows the airflow pattern inside the house (left side of fig.12) and airflow velocity region(less than 1 m/s, in between 1-2 m/s and higher than 2 m/s) inside the square shape house (right side of fig. 12) when the airflow direction is from south to north with different door/window orientations. In this part, the inflow air velocity is taken as 3.33 m/s. With N&E and N & W door/window configurations, the air volume flow rate is the lowest (3.55 m^3/s per unit door/window height) because the entire air enters through the main entrance door only. On the other hand, in the remaining door/window configuration it is 13.702 m^3/s per unit door/window height. With N & E door/window positioning, it is observed that a major fraction of air that enters through the main entrance door, moves out through the windows of the north side bedroom, toilet, and east side living room. A small amount of reverse flow air enters into the kitchen/dining space through all the windows provided. It is due to the adverse pressure formed by the main flow path. As previously discussed, recirculation zones are observed at the sides of the flow paths. Here a major portion of the area is covered with low velocity (< 1m/s). With N-W door/window positioning, all rooms positioned at south-west are poorly ventilated, even north side toilet as well. The cross-flow condition (N & S door/window configuration) is already disused in the previous section. With S & E door/window configuration, it is observed that the entire N-S region is ventilated poorly (< 1m/s) because a maximum fraction of air that enters from the south, travels towards the kitchen/dining area (N-E region). With S & W door/window configuration, the ventilation is found to be very nice inside the entire house. Very low percentage area covered with the low-velocity wind (< 1 m/s). The maximum area of the study room and kitchen/dining is under comfortable airflow conditions.

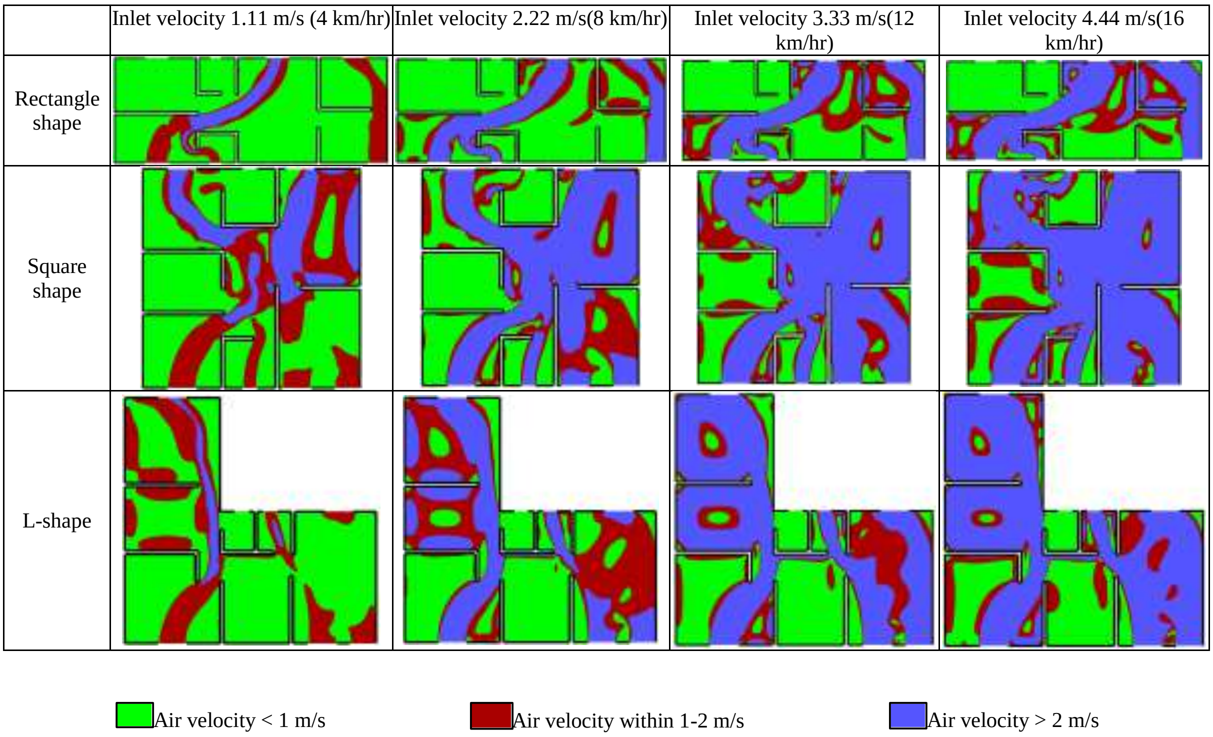

Figure 1.0 Air flow velocity region; less than 1 m/s (***green***), in between 1-2 m/s (***brown***) and higher than 2 m/s (***blue***) inside the house of various shapes, for different inlet airflow velocities with cross flow door/window orientation when airflow direction is from south to north.

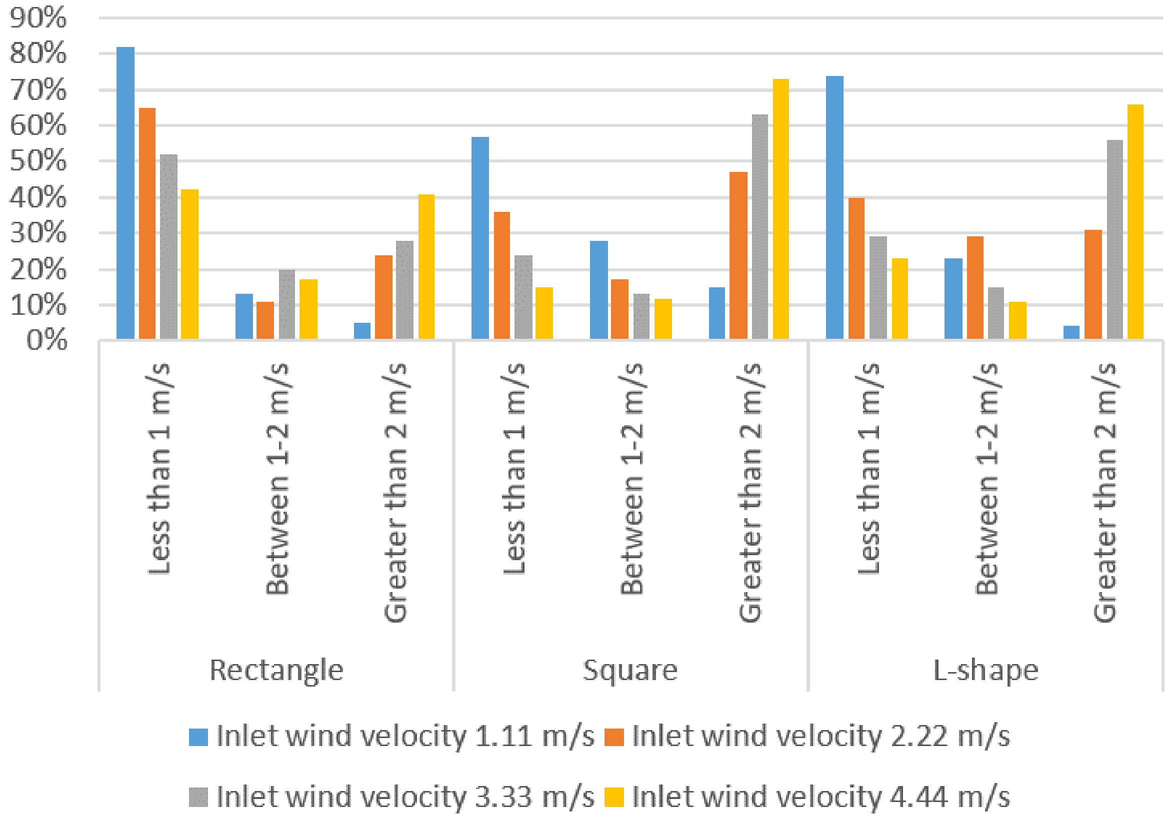

Figure 11. Air flow velocity covered the area in percentage inside the house of various shapes of the houses for different inlet airflow velocities with cross flow door/window orientation when airflow direction is from south to north.

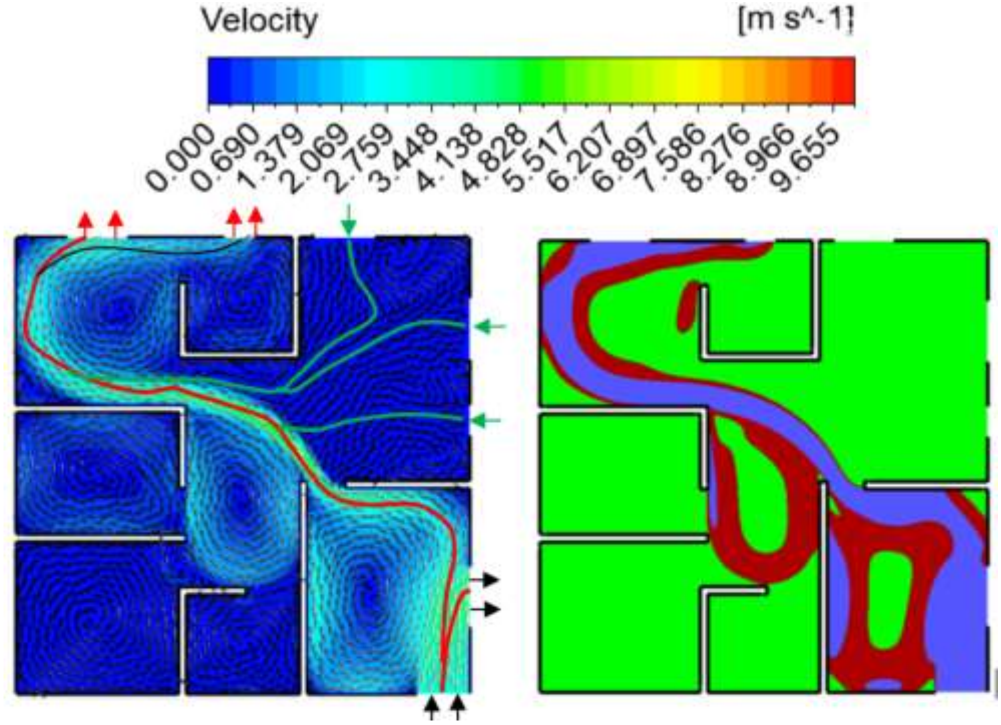

Velocity
[m s^-1]
0.000
0.690
1.379
2.069
2.759
3.448
4.138
4.828
5.517
6.207
6.897
7.586
8.276
8.966
9.655

(a)

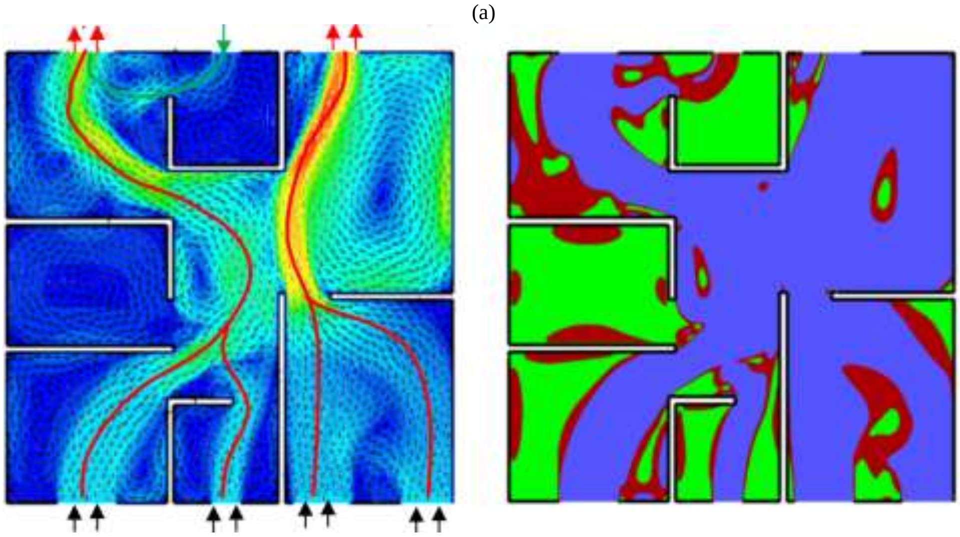

(b)

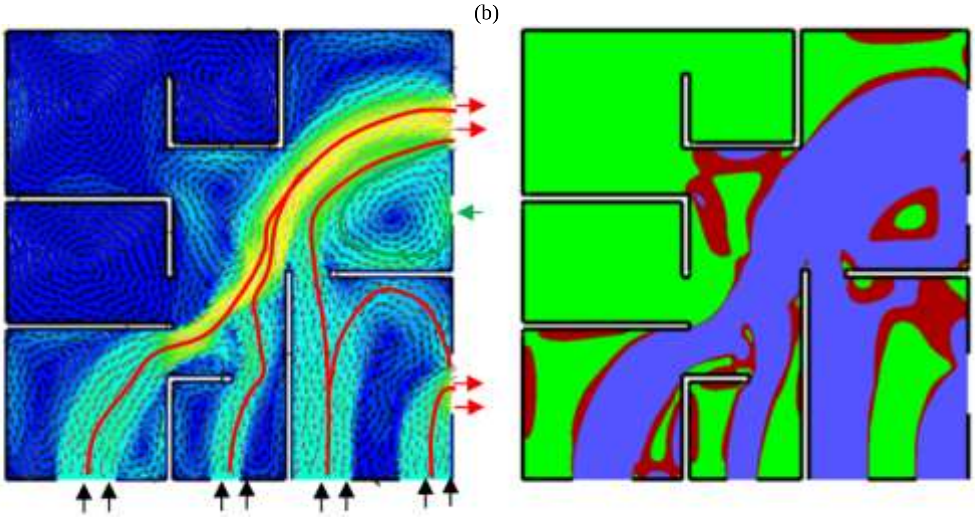

(c)

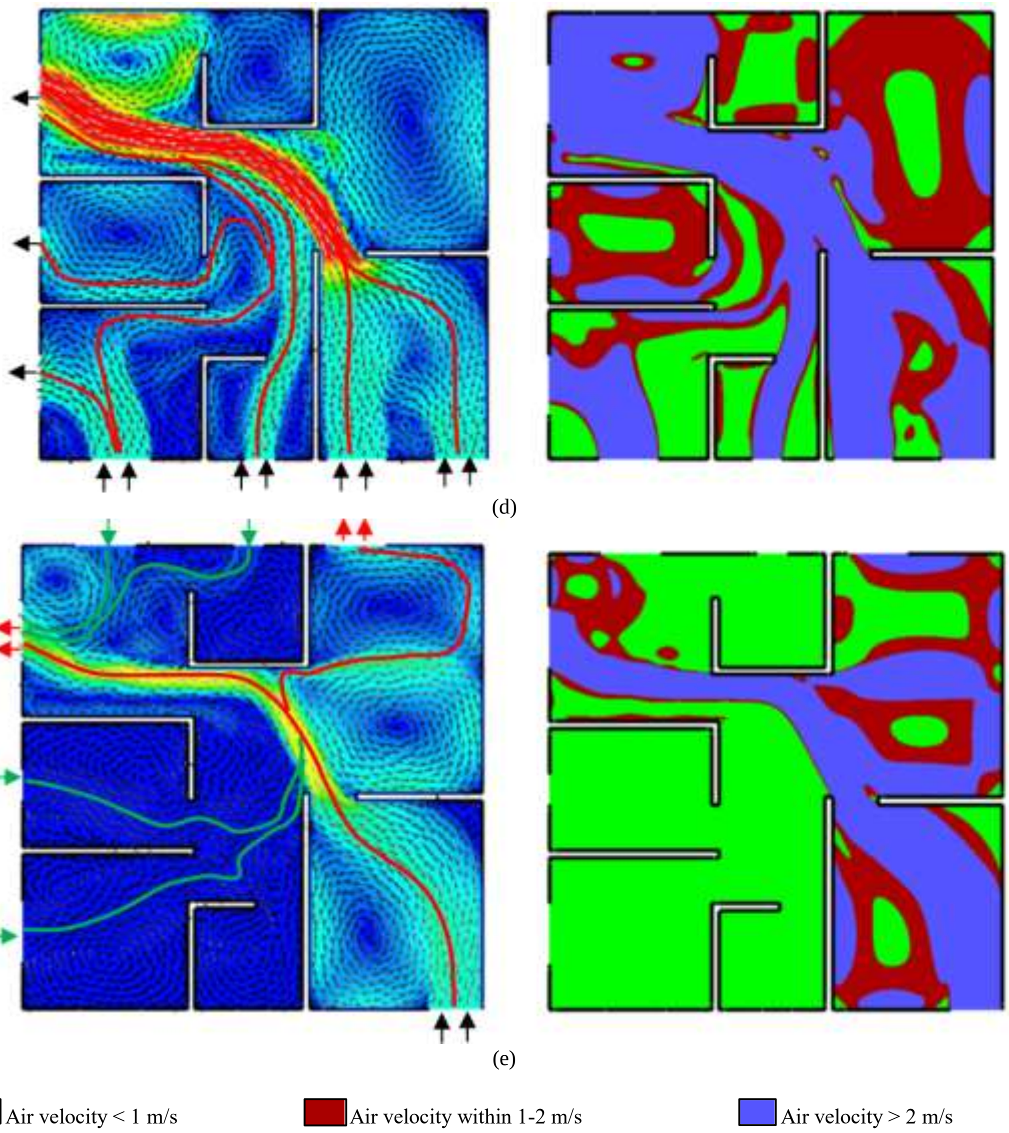

Figure 12. Airflow pattern inside the house (left) and airflow velocity region; less than 1 m/s (***green***), in between 1-2 m/s (***brown***) and higher than 2 m/s (***blue***) inside the house of rectangular shape (right) when the airflow direction is from south to north, for different door/window orientations (a) N & E opening (b) N & S opening (c) S & E opening (d) S & W opening (e) N & W opening

Figure 13 shows the airflow velocity region; less than 1 m/s (green colour region), between 1-2 m/s (browncolour region) and higher than 2 m/s (bluecolour region) inside the house of rectangular shape (right) with various airflow direction for different door/window orientations.The airflow inlet velocity is taken as 3.33 m/s.Figure 14 depicts the air flow velocity covering the area in percentage inside the house. It is observed that with N & Edoor/window configuration when the flow is from the south, 78% area of the house is covered with a low air velocity region (<1 m/s). It happens due to the low volume flow of air inlet. With S & W door/window configuration, when the flow is from the south, 27% area of the house is covered with comfort condition velocity region (between 1-2 m/s). Similarly, with N & S door/window configuration, when the flow is from the south, 63% area of the house is covered with the high-velocity region (> 2 m/s). It is because, in both S & W and N & S door/window arrangements, the airflow volume rate is higher.

Door/window orientation	Airflow from South	Airflow from north	Airflow from east	Airflow from west
N &W	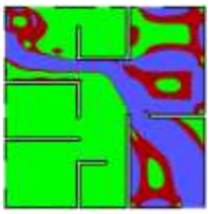		Not applicable due to closed wall	
N &S	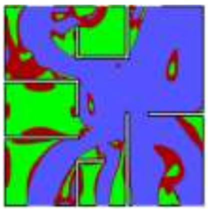	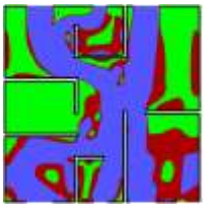	Not applicable due to closed wall	Not applicable due to closed wall
N &E		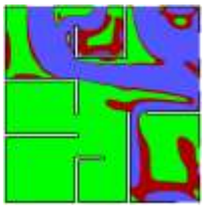	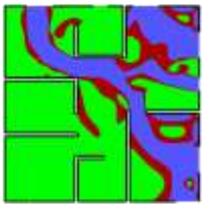	Not applicable due to closed wall
S &E		Not applicable due to closed wall		Not applicable due to closed wall
S &W	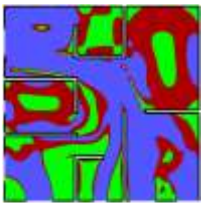	Not applicable due to closed wall	Not applicable due to closed wall	

Air velocity < 1 m/s Air velocity within 1-2 m/s Air velocity > 2 m/s

Figure 13. Air flow velocity region; less than 1 m/s (***green***), in between 1-2 m/s (***brown***) and higher than 2 m/s (***blue***) inside the house of rectangular shape,with various airflow directions for different door/window orientations, when airflow inlet velocity is 3.33 m/s.

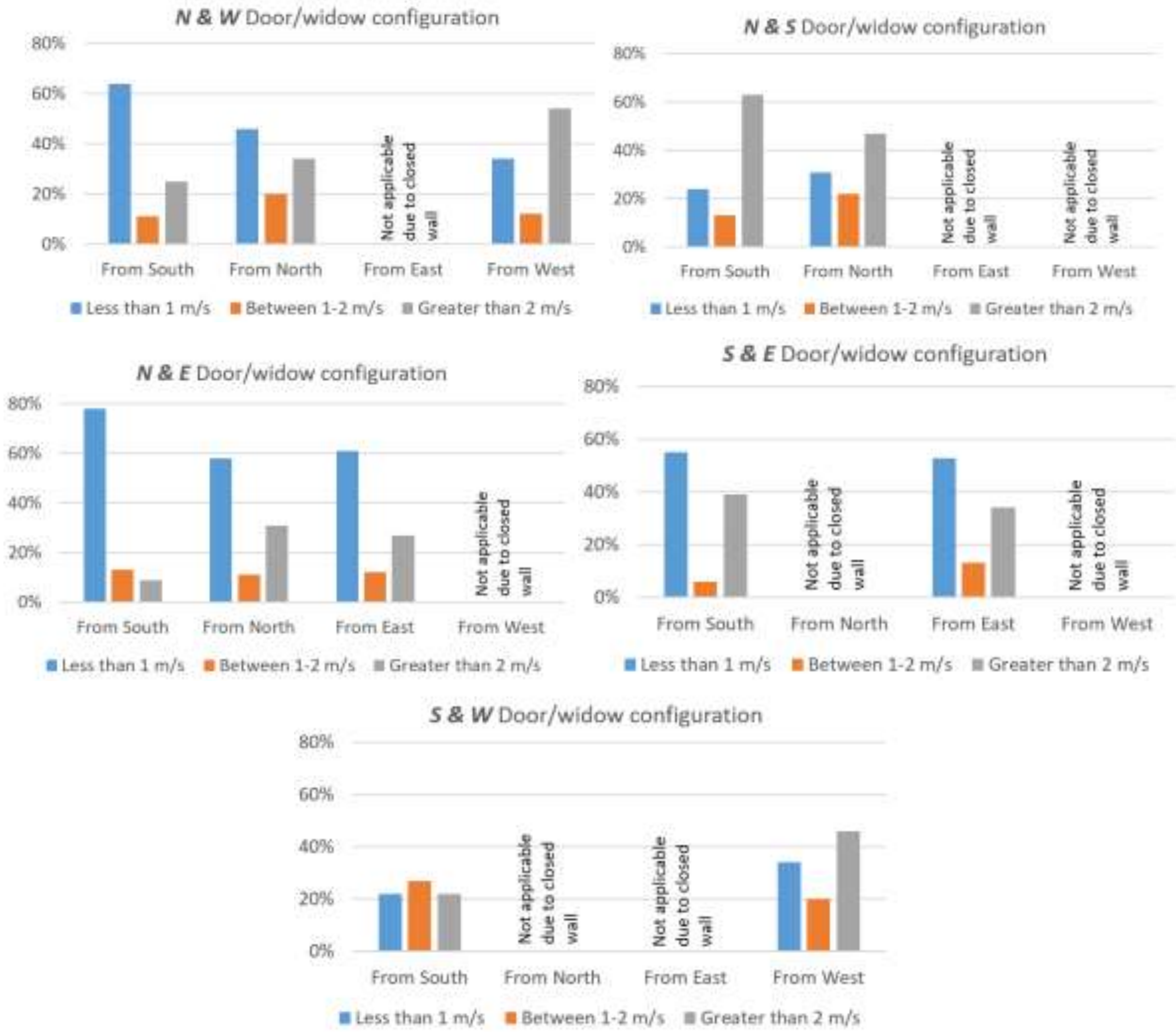

Figure 4. Air flow velocity covered the area in percentage inside the house of rectangular shape, with various airflow directions for different door/window orientations when airflow inlet velocity is 3.33 m/s.

5. Conclusion

Computational simulations have been performed to study the impact of partition walls on natural ventilation inside the house of various shapes and various door/window arrangments. The inflow air velocity range has been considered by following the 11-year wind data of Bhubaneswar city, India.Experimentation has also been performed to verify the predictional accuracy of the computational models used. The overall conclusion that has been drawn from the investigation is given as follows.

1. The volume of air inflow plays an important role in the airflow inside the house. With a single door/window entry, the volume of air inflow is less, hence there is poor ventilation observed.
2. With the increase in air flow inlet velocity, the area covered with low-velocity air (< 1 m/s) decreases and the area covered with high-velocity air (> 2 m/s) increases irrespective of the shape of the house. The area covered with comfort velocity (between 1-2 m/s) decreases with an increase in air inflow velocity for square shape houses and first increases then decreases in L-shaped houses but it does not follow any trend for the rectangular house.
3. For the given house size and door/window configuration, square shape house has the highest percentage area (63%) covered with higher velocity (> 2 m/s) and the rectangular shape house has the highest percentage area (52%) covered with lower velocity (<1 m/s) with south to the north wind flow direction. On the other hand, square shape house has a maximum of 22% area covered with comfortable airflow velocity (between 1-2 m/s) with north-to-south air flow direction.
4. Due to the low-pressure zone formed by the main air flow stream, some recirculation zone is observed near and around the main flow stream. Moreover, due to the same cause, some backflow is observed from some windows. The backflow is more prominent with a single door (main entrance door) air entry.
5. The airflow pattern does not vary significantly with an increase in inlet air velocity, but the various airflow velocity regions (velocity <1 m/s, > 1 m/s, and in between 1-2 m/s) inside the house are affected significantly. With the increase in inlet airflow

velocity, the fractional area of comfort airflow velocity and the high-velocity region increase.

6. With the N & E door/window configuration, for square shape house, the highest 78% area is covered with a low air velocity region (< 1 m/s). It happens due to low volume flow rate entry as air enters through only the main entrance door. With N & S door/window configuration, the highest 62% area is covered with a high air velocity region (> 2 m/s). It happens due to the high volume flow rate of air entry as air enters through windows and the main door.

References

[1] H. Sacht, M.A. Lukiantchuki, "Windows size and the performance of natural ventilation". J Procedia engineering. Vol. 196, No., 2017, 972-979.

[2] S. Ahmed, H. Mahammed, "A statistical analysis of wind power density based on the Weibull and Ralyeigh models of “Penjwen Region” Sulaimani/Iraq". Jordan Journal of Mechanical and Industrial Engineering. Vol. 6, No. 2, 2012, 135-140.

[3] J.E. Cermak, M. Poreh, J.A. Peterka, S.S. Ayad, "Wind tunnel investigations of natural ventilation". J Journal of transportation engineering. Vol. 110, No. 1, 1984, 67-79.

[4] L. Ji, H. Tan, S. Kato, Z. Bu, T. Takahashi, "Wind tunnel investigation on influence of fluctuating wind direction on cross natural ventilation". J Building Environment. Vol. 46, No. 12, 2011, 2490-2499.

[5] J.K. Calautit, B.R. Hughes, "Wind tunnel and CFD study of the natural ventilation performance of a commercial multi-directional wind tower". J BuildingEnvironment. Vol. 80, No., 2014, 71-83.

[6] A. Tecle, G.T. Bitsuamlak, T.E. Jiru, "Wind-driven natural ventilation in a low-rise building: A Boundary Layer Wind Tunnel study". J Building Environment. Vol. 59, No., 2013, 275-289.

[7] J. Cho, C. Yoo, Y. Kim, "Effective opening area and installation location of windows for single sided natural ventilation in high-rise residences". J Journal of Asian Architecture Building Engineering. Vol. 11, No. 2, 2012, 391-398.

[8] S. Omrani, V. Garcia-Hansen, B.R. Capra, R. Drogemuller, "Effect of natural ventilation mode on thermal comfort and ventilation performance: Full-scale measurement". J Energy Buildings. Vol. 156, No., 2017, 1-16.

[9] E. Kyritsi, A. Michael, "An assessment of the impact of natural ventilation strategies and window opening patterns in office buildings in the mediterranean basin". J Building Environment. Vol. 175, No., 2020, 106384.

[10] E. Dascalaki, M. Santamouris, A. Argiriou, C. Helmis, D. Asimakopoulos, K. Papadopoulos, A. Soilemes, "Predicting single sided natural ventilation rates in buildings". J Solar Energy. Vol. 55, No. 5, 1995, 327-341.

[11] S. Hawendi, S. Gao, "Impact of an external boundary wall on indoor flow field and natural cross-ventilation in an isolated family house using numerical simulations". J Journal of Building Engineering. Vol. 10, No., 2017, 109-123.

[12] X. Zhang, A.U. Weerasuriya, J. Wang, C.Y. Li, Z. Chen, K.T. Tse, J. Hang, "Cross-ventilation of a generic building with various configurations of external and internal openings". J Building Environment. Vol. 207, No., 2022, 108447.

[13] Z. Zhiyi, Y. Wei, W. Tianwen, L. Yonghan, Z. Yawen, Z. Guoqiang, "Potential of cross-ventilation channels in an ideal typical apartment building predicted by CFD and multi-zone airflow model". J Journal of Building Engineering. Vol. 44, No., 2021, 103408.

[14] J.O. Cheung, C.-H. Liu, "CFD simulations of natural ventilation behaviour in high-rise buildings in regular and staggered arrangements at various spacings". J Energy Buildings. Vol. 43, No. 5, 2011, 1149-1158.

[15] R.N. Meroney, CFD prediction of airflow in buildings for natural ventilation, in: Proceedings of the Eleventh Americas Conference on Wind Engineering, Puerto Rico, 2009.

[16] T. van Hooff, B. Blocken, L. Aanen, B. Bronsema, "A venturi-shaped roof for wind-induced natural ventilation of buildings: wind tunnel and CFD evaluation of different design configurations". J Building Environment. Vol. 46, No. 9, 2011, 1797-1807.

[17] S. Derakhshan, A. Shaker, "Numerical study of the cross-ventilation of an isolated building with different opening aspect ratios and locations for various wind directions". J International Journal of Ventilation. Vol. 16, No. 1, 2017, 42-60.

[18] S. Liu, W. Pan, Q. Cao, Z. Long, Y. Jiang, Q. Chen, "CFD simulations of natural cross ventilation through an apartment with modified hourly wind information from a meteorological station". J Energy Buildings. Vol. 195, No., 2019, 16-25.

[19] M.-F. King, H.L. Gough, C. Halios, J.F. Barlow, A. Robertson, R. Hoxey, C.J. Noakes, "Investigating the influence of neighbouring structures on natural ventilation potential of a full-scale cubical building using time-dependent CFD". J Journal of Wind Engineering Industrial Aerodynamics. Vol. 169, No., 2017, 265-279.

[20] K. Visagavel, P. Srinivasan, "Analysis of single side ventilated and cross ventilated rooms by varying the width of the window opening using CFD". J Solar Energy. Vol. 83, No. 1, 2009, 2-5.

[21] J. Wang, S. Wang, T. Zhang, F. Battaglia, "Assessment of single-sided natural ventilation driven by buoyancy forces through variable window configurations". J Energy buildings. Vol. 139, No., 2017, 762-779.

[22] L.K. Moey, M.F. Kong, V.C. Tai, T.F. Go, N.M. Adam, "Effect of Gable Roof Angle on Natural Ventilation for an Isolated Building". Jordan Journal of Mechanical and Industrial Engineering. Vol. 15, No. 3, 2021.

[23] C. Allocca, Q. Chen, L.R. Glicksman, "Design analysis of single-sided natural ventilation". J Energy buildings. Vol. 35, No. 8, 2003, 785-795.

[24] Y. He, Y. Chu, H. Zang, J. Zhao, Y. Song, "Experimental and CFD study of ventilation performance enhanced by roof window and mechanical ventilation system with different design strategies". J Building Environment. Vol., No., 2022, 109566.

[25] M. Liu, C. Jimenez-Bescos, J. Calautit, "CFD investigation of a natural ventilation wind tower system with solid tube banks heat recovery for mild-cold climate". J Journal of Building Engineering. Vol. 45, No., 2022, 103570.

[26] T.K. Sahoo, P. Ghose, "Effect of Inlet Swirl on Combustion Performance and Soot Formation of a Turbulent Methane-Air Non-Premixed Flame". Jordan Journal of Mechanical and Industrial Engineering. Vol. 16, No. 2, 2022.

[27] Ali M. Jawarneh, G.H. Vatistas, "Reynolds stress model in the prediction of confined turbulent swirling flows". Vol., No., 2006.

[28] Ali M. Jawarneh, "Heat transfer enhancement in a narrow concentric annulus in decaying swirl flow". J Heat Transfer Research. Vol. 42, No. 3, 2011.

[29] Ali M. Jawarneh, M. Al–Widyan, A. Al–Migdady, H. Tlilan, M. Tarawneh, A. Ababneh, "Double vortex generators for increasing the separation efficiency of the air separator". J INTERNATIONAL JOURNAL OF HEAT TECHNOLOGY. Vol. 35, No. 3, 2017, 529-538.

[30] M. Khan, I. Janajreh, "Transevaporative Cooling Performance of a Three-Sided Wind Catcher". J Jordan

Journal of Mechanical Industrial Engineering. Vol. 11, No. 4, 2017.

[31] Z.M. Wawrzyniak, G. Borowik, E. Szczechla, P. Michalak, R. Pytlak, P. Cichosz, D. Ircha, W. Olszewski, E. Perkowski, Relationships between crime and everyday factors, in: 2018 IEEE 22nd International Conference on Intelligent Engineering Systems (INES), IEEE, 2018, pp. 000039-000044.

[32] O. Shaalan, H.M.A. Gad, M.I. Riad, "Comparison of Antibacterial Effect of Probiotic Yogurt and Xylitol-Containing Chewing Gum in Geriatric Patients: A Randomized Controlled Clinical Trial". J Acta Stomatologica Croatica. Vol. 55, No. 4, 2021, 380.